Characterization of Ashes from Different Wood Parts of Norway Spruce Tree

Liang Wang*[a], Janka Dibdiakova[b]

[a]SINTEF Energy Research, Sem Sælands vei 11, Trondheim, Norway
[b]Norwegian Forest and Landscape Institute, NO-1431, Ås, Norway
liang.wang@sintef.no

Woody biomass from the forest sector is an abundant resource for renewable energy generation. Conventional woody biomass materials such as timber and stem are normally high quality solid fuels for combustion applications in terms of ash related operational problems. Recently, new raw woody materials such as forest residue are gaining interests for energy production purpose. Forest residue is the remaining fraction after harvest and outtake of the wood timber, including tree tops, branches and barks. Compared to conventional woody biomass, the forest residue has a wide variation of ash content and concentration of ash forming matters. The aim of this work was to characterize and investigate different parts from Norway spruce trees regarding ash content, ash composition and ash melting and slagging behaviors. Different parts from spruce tree were studied in present work including stem wood, bark, branch and twigs. The ash content and ash melting temperature of the four fuel samples were measured through following standard procedures. Concentrations of main ash forming elements were analyzed by an inductively coupled plasma optical emission spectroscopy (ICP-OES). The ashes from stem wood, bark and twigs were further investigated by a scanning electron microscopy equipped with energy dispersive X-Ray analysis (SEM-EDX) and X-Ray diffractometry (XRD). The results showed that the branches and twigs contain higher contents of ash forming matters than that of the stem wood. Chemical compositions of ashes from four parts of the spruce tree are dominated by Ca, K, and Si. The K and Na contents in the branches and twigs are significantly higher than that of stem wood and bark, indicating high tendency of ash melting and slagging. The melting points of ashes from branch and twigs were 100-200 °C lower than those of the ashes from stem wood and bark, respectively. SEM-EDX and XRD analysis, melting of ashes from branch and twigs are mainly attributed to formation and fusion of low temperature melting alkali silicates.

1. Introduction

Utilization of woody biomass for heat and power production has been mainly restricted to timber, sawdust, wood chips and shavings from sawmills and wood working industry (Boström et al., 2011). However, with the rapid increase of demand of bioenergy, woody biomass materials from forest residues are gaining continuous interests recently. Forest residues are derived from harvest of forests and outtake of timber process. In Norway, 37% of the Norwegian mainland is covered by forest (119,000 Km^2). About 1.5 million m^3 are produced annually in Norway with large amounts available for energy production. Norway has set a goal to produce new 14 TWh bioenergy by 2020, and extend use of forest residues will certainly help to meet the goal (Liang et al., 2013). With development of collecting and bundling technologies, the efficient recovery and utilization of the forest residues become more important. Currently, combustion is still the most widely used technology for converting woody biomass into heat and power (Liang et al., 2013). However, as a group of solid fuel for combustion applications, in contrast to ordinary woody biomasses, the forest residues have large variations in total fuel ash content and composition of ash forming elements (Werkelin et al., 2005). Therefore, the ash transformation chemistry during combustion of forest residues may be considerably different than those of conventional woody biomass fuels (Ehsan et al., 2013). In previous studies, ashes in pure sample of stem wood, bark and foliage from trees of pine, spruce, birch

and aspen were analysed. Both total fuel ash content and concentrations of ash forming elements are significantly different for three parts of each tree species (Werkelin et al., 2010). Compared to stem wood sample, the foliage contains much higher contents of ash and elements such as K, P and S (Werkelin et al., 2011). Due to rather higher contents of fuel ash and critical ash forming elements in forest residues, ash related problems such slagging and fouling are expected to occur during combustion process (Öhman et al., 2004). Such ash related operational problems may cause unscheduled shutdowns and costly maintenances of combustion appliances (Lindström et al., 2010). It was stated that ash rich bark and logging residues have high ash sintering tendency, which resulted in severe slagging problems during combustion in different types of burners (Lindström et al., 2010). Ashes from combustion of the bark and logging residues were investigated via a combination of different analytical methods. The analysis results revealed that ash slagging tendency correlated well to content of Si and K in the fuel (Öhman et al., 2004). Formation and melting of different alkali silicates is one of main reasons leading ash sintering and slagging (Wang et al., 2011). However, because of large heterogeneity of forest residues, the knowledge of ash characteristics is still limited.

The objectives of the present work were: 1) characterization of ashes from different parts of Norway spruce tree, 2) investigation the studied fuel ash melting and sintering behaviours at elevated temperatures, 3) studying the ash sintering chemistry through a combination of XRD and SEM-EDX analysis.

2. Experimental section

The stem wood and forest residues were obtained from a Norway spruce forest in East Norway (Hobøl, Latitude 59°43 'N and Longitude 10°52 'E). The Norway spruce tree were first cut down and divided into four parts along the tree trunk from base level, bottom crown level, middle crown level and top crown level. The stem wood, stem bark, branches and twigs from each level were separated afterwards. Along the stem to needle top radial direction, the branch was divided into four parts including base section, middle section, top section and needle top. All fuel samples were collected and air dried first, which were milled to particle size smaller than 1 mm and dried again at 105 °C to get stable weight. The ash content of each fuel sample was measured through following ASTM standard D 1102. Chemical compositions of each ash sample were analyzed by an inductively coupled plasma optical emission spectroscopy (ICP-OES). The samples for ICP-OES analysis were prepared by following the standard CEN-TS 15920. About 50 mg ash sample produced at 550 °C was digested by a mixture of acid H_2O_2, HNO_3 and HF in the first stage, and H_3BO_3 in the second stage. The melting temperature of one 550 °C ash sample was measured according to procedures described in the standard. ISO 540: 1995. Each ash sample was first shaped into a cubical specimen. The ash specimen was then put in an ash fusion analyzer, in which it was heated from room temperature to 1,500 °C at a heating rate of 2 °C/min in an oxidizing atmosphere. Shape changes of the ash specimen at elevated temperatures were recorded, which were used for determine ash fusion characteristic temperatures. Four ash fusion characteristic temperatures were determined including initial deformation temperature (IDT), softening temperature (ST), hemisphere temperature (HT) and fluid temperature (FT). For each ash sample, 6 tests were performed and the average test values are presented in Table 3.

In addition, 50 g of each fuel sample was burned at 1000 °C for 5 h. After combustion, the ash residues from each fuel sample were visually evaluated in terms of sintering degree. Part of the ash residues were analyzed by a Bruker D8 Advance X-ray diffractometer using Cu k-alpha radiation and a LynxEye detector. Identification of the crystalline components in each sample was done through an instrument integrated TOPAS evaluation program and the ICDD-PDF2 database. In addition, the ash residues from four fuel samples were analyzed by scanning electron microscopy (SEM) equipped with Energy Dispersive X-ray spectrometry (EDX). The ash residue samples were collected and stick on a carbon tape on a sample holder. The SEM was operated in a backscattered electron mode for illustrating distribution of detected elements in a scanned area. EDX semi-quantitative spot/area analyses were carried out for interesting areas to get more detailed microchemistry information.

3. Results and discussion

3.1 Ash content
Ash contents of each part of the Norway spruce tree are presented in Table 1. The ash content in the stem wood was 0.18-0.2 %. The ash content of the bark was 1.49-2.11 %, which is 8-10 times of those of the corresponding stem wood. The branch and top have high ash contents about 1.17-1.89 %.

Table 1: Ash content of fuel samples from different parts from a summer harvest Norway spruce tree

Ash content (wt %. db[a])	Stem wood	Stem Bark	Branch and top			
			base	Middle	top	Needle top
Base level	0.18	1.49	[b]	[b]	[b]	[b]
Bottom crown level	0.19	1.65	1.17	1.28	1.41	1.69
Middle crown level	0.20	2.11	1.22	1.34	1.56	1.79
Top crown level	0.20	1.96	1.32	1.50	1.69	1.89

a: dry basis; b: not detected.

Table 1 shows that the ash content of fuel samples from different parts of tree increased along trunk of the tree. The ash contents of fuel samples from higher level crown are evidently higher than those of lower part of the living crown. The similar correlation between the ash content and parts of the tree was reported (Werkelin et al., 2005). In addition, along the whole branch, the ash content of each sample category increased, and the highest ash content was in the needle top. In previous study, higher ash contents were also measured from the needles and shoots of four tree species, which well-resembled the results showed in Table 1.

3.2 Ash forming elements

The wood discs containing stem wood and bark were cut from the tree. The stem wood and bark were separated afterwards. Branches and twigs were collected from the same tree height level. The branches contain large size branches that are from base and middle section of the branches. The twigs refer to thinner branches together with attached foliage and needles. The concentration of main ash forming elements in each fuel samples from each part of the tree along the radical direction. As shown in Table 2, the stem wood sample has the lowest concentrations of all ash forming elements. The dominating element in the stem wood ash (550 °C) is Ca, K and Mn. The stem bark ash has the similar chemical compositions as those of the stem wood, but the significant higher amounts of Si, P and Al. The branches contained both wood and bark parts, and the concentrations of elements Ca, Al, Zn and Mn are between those of stem wood and bark as shown in Table 2. However, the Si content in the branch ash is significantly higher than those of the ashes from stem wood and bark. The ash produced from the twigs is dominated by Ca, Si, K, P and Mn. The concentrations of element Si, K and P are much higher than those in ashes from the stem wood, bark and branch. The contents of Si, K, P, and S in the ashes from the four fuel samples increased in the order stem wood < stem bark < branch < twigs. The twigs have considerably high contents of Si, K and P, which were 100, 15 and 50 times higher than those in the stem wood ash, respectively. The K, P and S are mobile elements as reported in literatures of plant physiology (Werkelin et al., 2010). They readily solve in sap solutions and are rich in the young and biologically active issues. High concentrations of K, P and S in parts of the tree (e.g. foliage and shoots) have been reported (Werkelin et al., 2010). These parts of the tree contain a large amount of living cells and high content of K and P as well. On the other hand, the Ca and Mn are characterized as rather immobile elements that accumulate easily in the phloem sap, a major composition of the bark. It could explain the high concentrations of Ca and Mn in the stem bark. In addition, the branch contains both bark and wood, which is rich in Ca and Mn as shown in Table 2. Si is likely to solve in the certain phloem sap in the tree tissue, which keeps contact with air (Werkelin et al., 2005). Twigs part of the tree/branch is such kind of tissue, which explains that has the highest Si content among four parts of the tree. The large variations of ash forming elements in different parts of the one spruce tree species have been reported (Werkelin et al., 2010). The similar concentrations of ash forming elements in different parts of a tree were also observed from the other three tree species pine, birch and aspen in the same study.

3.3 Ash melting and sintering behaviours

The ash melting and sintering behaviors of ashes from four parts of the spruce tree were investigated. Firstly, the melting temperatures of ashes from the four parts (stem wood, bark, braches and twigs) produced at 550 °C were measured and the results are shown in Figure 1.

Table 2: Concentrations of major ash forming elements (mg/Kg D.S.) in fuels samples

Sample	Ca	Si	K	Na	Al	P	S	Mg	Fe	Zn	Mn
Stem wood	25,742	433	8,752	8,106	127	975	929	670	79	446	2,758
Stem bark	221,064	8,147	70,668	6,217	3,086	25,359	9,710	7,769	924	5,054	18,284
Branch	163,671	26,673	85,830	5,403	2,541	31,290	11,873	4,461	1,111	4,758	16,032
Twigs	120,663	58,220	128,051	3,564	1,646	52,197	13,320	3,615	695	1,486	12,511
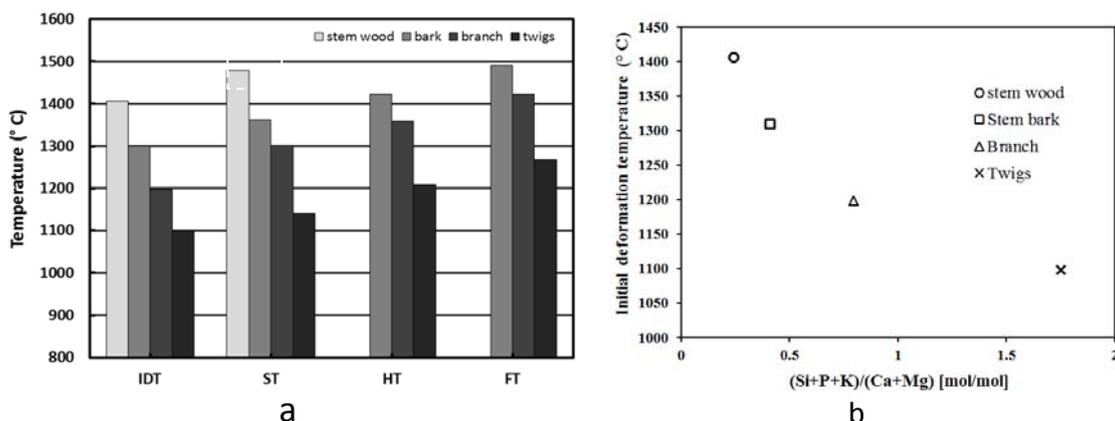
Figure 1: a) Ash fusion characteristic temperature of ashes from four parts of the spruce tree, b)

The initial deformation temperature is more interesting, since one ash starts to melt and become sticky, causing ash related operational problems. As Figure 1 shows, the stem wood ash has the highest initial melting temperature, indicating the lowest sintering tendency. During the ash fusion test, only the ash initial deformation temperature was identified at about 1,400 °C. The other three ash fusion characteristic temperatures (ST, HT and FT) were not able to be measured, since not evident shape changes were hard to be observed at elevated temperatures. The ash fusion test results from the stem wood agreed with observed results from combustion tests. The stem wood ash has an evidently porous structure without observation of sintering and melting. On the contrary, the ash from twigs has the lowest ash initial deformation temperature about 1,100 °C that is considerably lower than those of the other three ashes. As the temperature higher than 1,100 °C, the swelling and bubbling of the twig ash were observed, indicting the ash was passing through sever molten stage and behaved as liquid. After measuring the ash fusion temperature, the ash specimen melted completely and residues left as a thin layer. After the fuel combustion test, even no sintering, the slightly aggregation of twig ash grains was already observed.

Microscopic observation showed variations of particle shape, structure and morphology of all ash residues after fuel combustion at 1,000 °C. Figure 2 shows one representative SEM image of stem wood ash with porous structures. The ash residue contains long flakes like grains and some small particles with irregular shapes. The former one is probably the ash left combustion of wood tissue, which somehow keeps tissue like structure with layers and pores as shown in Figure 2-b. From the flake like particle, Ca was detected as a dominating element with small amount of Mg and Mn. Therefore, detection of these elements implies presence of metal oxide, which was confirmed by XRD analysis (Table 3). However, from the small irregular particles, rather a small amount of S was also detected, with detection of Ca as a major element in the same area. The strong correlation between the S and Ca can be found from the EDX element mapping indicating formation of $CaSO_4$ in the stem wood ash. The stem bark ash is comprised of medium and small sized particles as shown in Figure 3-a. Some of ash grains have porous structures with small pores on the surface. Elements Ca, K and P were detected from the porous ash grains, indicating presence of potassium calcium phosphates. On the other hand, there are some cubical grains can be observed from the larger ash grain surfaces as shown in Figure 3-b. Over than 95 wt% of calcium was detected from these cubical grains ($\geq$ 20 µm). Therefore these grains are small Ca rich crystals that were detected by XRD analysis (Table 3). The similar calcium rich crystals in the bark ash have been observed and reported by Werkelin et al (Werkelin et al., 2011). During the burnout stage, the calcium dispersed in char structure will diffuse to char particle surface as small crystallites. With further migration and coalescence, large calcium rich crystals will form and sintered together as shown in Figure 3-b. Figure 4 displays the twig ash contains two kinds of grains in terms of morphology and structure. Some of ash grains appeared as large fused, homogenous structures with minor ash particles embed. The K and Si were detected as main elements from the fused portion that are melted potassium silicates accordingly. The fused silicates in the ash that explains presence of amorphous phase materials as revealed by XRD analysis, which appears as a hump in the base line of the spectrum of the twig ash. Due to the high concentration of K and Si in the twig, different potassium silicates readily form during the combustion process. Some of potassium silicates have melting points as low as 600 °C. Formation and melting of the potassium silicates make the ash grains sticky and aggregate, initiating ash sintering and slagging consequently. It has been reported that K-silicates chemistry plays a main role for ash slagging during combustion of K and Si rich forest assortments such as needle and thinning from trees (Werkelin et al.,

2011). In addition, K in the biomass fuel has a high affinity to react with P during combustion processes. It leads to formation of low temperature melting K-phosphates that may melt and promote sintering of the biomass ash (Boström et al., 2011). As the K-silicates melts encounter alkali earth metals Ca and Mg, the Ca and Mg may dissolve into the melts and drive out the K (Boström et al., 2011). As a result of this, the amount of K-silicates melts will reduce and sintering degree of the ash as well. Moreover, Ca and Mg in biomass ash will also incorporate into the K-phosphate, enhancing formation of K-Ca-phosphates with high melting temperatures. Therefore, as the Ca and Mg content increase, the ash melting points is also increasing. Figure 2-b shows a good correlation between concentrations of key ash forming elements (indicated as a mole ratio between Si+K+P/Ca+Mg) with the ash fusion temperature.
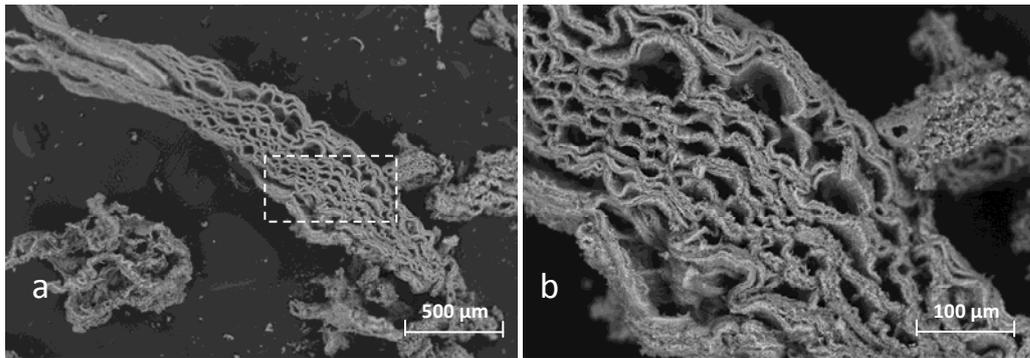
Figure 2: SEM image of stem wood ash produced at 1000 °C
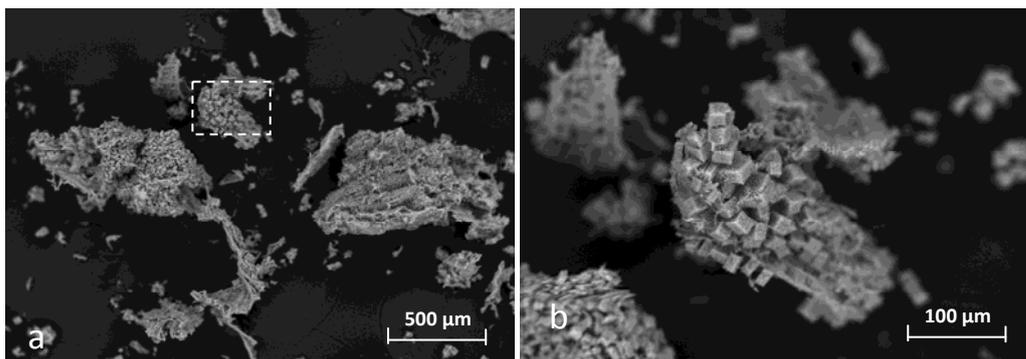
Figure 3: SEM image of stem bark ash produced at 1000 °C
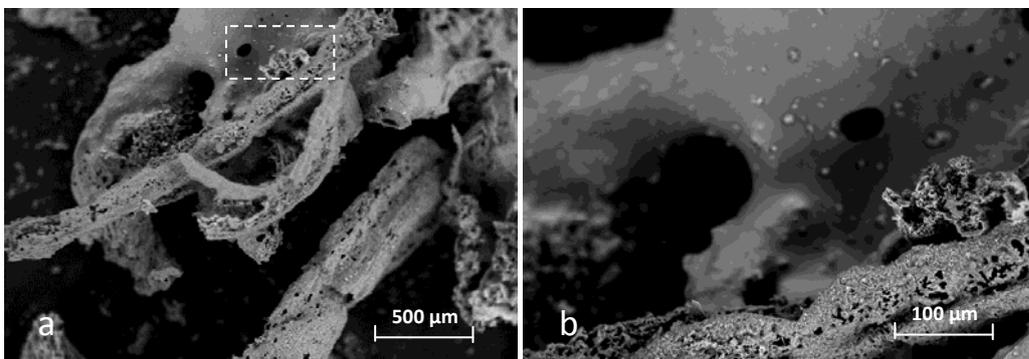
Figure 4: SEM image of twigs ash produced at 1000 °C

42

Table 3: Major mineral phases observed from barley straw ash with and without additive addition

Major mineral phases	
Stem wood ash	CaO, MgO, trace amount $CaSO_4$
Stem bark ash	CaO, MgO, $Ca_5(PO_4)_3$, small amount $CaSiO_3$,
Branch ash	K_2SO_4, $Ca_5(PO_4)_3$, $CaSiO_3$, CaO, MgO
Twig ash	$CaSiO_3$, $Ca_5(PO_4)_3OH$, $CaMgSi_2O_6$, MgO, trace amorphous material

4. Conclusions

The ash contents of different parts from the Norway spruce tree are different. Compared to the stem wood, the bark, branch and twig containing a large amount living tissues generally have higher ash content. In addition, concentrations of ash forming elements in different parts of the Norway spruce tree are significantly different. Contents of Si and K are low in the stem wood, but can be considerably higher in the twig. The ash from the studied twig showed high sintering tendency due to high content of fuel ash and certain ash forming elements such Si and K. The SEM-EDX together with XRD analyses indicated that melting of the twig ash is mainly due to formation of low temperature melting potassium silicates. Thus, the large variation of major ash forming elements in different parts of the tree should be considered for a more efficient combustion of different wood biomasses for combustion applications.

Acknowledgement

The authors acknowledge the financial support by the Bioenergy Innovation Centre (CenBio), which is funded by the Research Council of Norway, a large number of industry partners and seven R&D institutions.

References

Boström D., Skoglund N., Grimm A., Boman C., Öhman, M., Broström M., Backman R., 2011, Ash Transformation chemistry during combustion of biomass, Energy Fuels, 26(1), 85-93.

Wang L., Sandquist J., Varhegyi G., Matas Güell B., 2013, CO_2 Gasification of Chars Prepared from Wood and Forest Residue: A Kinetic Study, Energy & Fuels, 27, 6098-6107.

Wang L., Becidan M., Skreiberg, O. 2013, Testing of Zeolite and Kaolin for Preventing Ash Sintering and Fouling during Biomass Combustion. Chemical Engineering Transactions, 35.1159-1164.

Werkelin J., Skrifvars B.-J., Hupa M., 2005, Ash-forming elements in four Scandinavian wood species. Part 1: Summer harvest, Biomass and Bioenergy, 29, 451-466.

Werkelin J; Lindberg, D; Boström D., Skrifvars B.-J., Hupa M., 2011, Ash-forming elements in four Scandinavian wood species part 3: Combustion of five spruce samples, Biomass and Bioenergy, 35, 725-733.

Houshfar E., Wang L., Vähä-Savo N., Brink A., Løvås T. 2013, Experimental Study of a Single Particle Reactor at Combustion and Pyrolysis Conditions. Chemical Engineering Transactions, 35. 613-618.

Werkelin J., Skrifvars B.-J., Zevenhoven M., Holmbom B., Hupa M., 2010, Chemical forms of ash-forming elements in woody biomass fuels, Fuel, 89, 481-493.

Öhman M., Boman C., Hedman H., Nordin A., Boström D., 2004, Slagging tendencies of wood pellet ash during combustion in residential pellet burners, Biomass and Bioenergy, 27, 585-596.

Lindström E., Larsson S.H., Boström D., Öhman M., 2010, Slagging Characteristics during Combustion of Woody Biomass Pellets Made from a Range of Different Forestry Assortments, Energy Fuels, 24, 3456-3461.

Wang L., Skjevrak G., Hustad J., Grønli M., 2011, Effects of Sewage Sludge and Marble Sludge Addition on Slag Characteristics during Wood Waste Pellets Combustion, Energy Fuels, 25, 5775-5785.

Wu H., Castro M., Jensen P.A., Frandsen F.J., Glarborg P., Johansen Dam K. , Røkke M., Lundtorp K., 2001, Release and Transformation of Inorganic Elements in Combustion of a High-Phosphorus Fuel, Energy Fuels, 25, 2874-2886.